Optical stimulated nutation echo

Szabo, A.; Shakhmuratov, R. N.

Publisher's version / Version de l'éditeur:
https://doi.org/10.1103/PhysRevA.55.1423
Physical Review A, 55, 2, pp. 1423-1429, 1997-02-01

Optical stimulated nutation echo

A. Szabo
Institute for Microstructural Sciences, National Research Council of Canada, Ottawa, Ontario, Canada K1A 0R6

R. N. Shakhmuratov*
Kazan Physical-Technical Institute, Russian Academy of Sciences, 10/7 Sibirsky Trakt Street, Kazan 420029, Russia

(Received 1 August 1996)

Observation of the optical analog of the delayed nutation echo [V. S. Kuz'min *et al.*, Zh. Éksp. Teor. Fiz. **99**, 215 (1991) [Sov. Phys. JETP **72**, 121 (1991)] recently shown in nuclear magnetic resonance is reported. We call this echo a *stimulated nutation echo* (SNE) in analogy to the three-pulse-stimulated echo that is produced from a hole pattern burnt into an inhomogeneous line. In a SNE two-pulse sequence, the first pulse burns a train of holes into the inhomogeneous absorption spectrum and its duration t_p is stored. After a long delay time the second pulse burns its own train of holes. When coincidence of these holes takes place, the SNE occurs at a time $t=t_p$ following the start of the second pulse. Thus the second pulse reads exactly the duration of the first pulse. It is shown that for a Gaussian-shaped beam, the echo becomes sharper and well recognizable. This echo may be used for Rabi frequency measurement and spectral diffusion studies. [S1050-2947(97)01302-4]

PACS number(s): 42.50.Md, 76.60.Lz

I. INTRODUCTION

Optical nutation is a commonly used, simple method of Rabi frequency measurement for ions excited by a laser [1–5]. The Rabi frequency contains useful information about transition dipole matrix elements as well as the driving field amplitude. Delayed nutation [5–9] is an extension of this method for the measurement of population difference relaxation time T_1. In this paper we consider a different nutation effect, the stimulated nutation echo (SNE), the optical analog of an echo recently seen in nuclear magnetic resonance [10], which combines the possibility of measurement of both Rabi frequency and T_1 simultaneously. This method provides better resolution for Rabi frequency measurement as the SNE has 2.6 times larger amplitude than the transient nutation signal. Moreover, it allows the study of spectral diffusion in solids, similar to the three-pulse-stimulated echo.

II. THEORY

We consider the effect of a two-pulse sequence resonant with an ensemble of two-level particles. Pulse I of duration t_p burns a train of holes in the inhomogeneous absorption spectrum of the sample. The structure of the hole train is determined by the product χt_p, where χ is the Rabi frequency. After a delay time t_d, the long pulse II starts to excite its own train of holes. When the Rabi frequency is the same for both pulses, the second hole train coincides with the first exactly at a time $t=t_p$, where t is measured from the beginning of pulse II. Interference of the holes produces a two-component hole in the absorption spectrum. The first component is smooth and does not contain oscillations in the frequency domain at $t=t_p$. The second component has a doubled frequency of oscillations. The particles' response on the driving field depends strongly on their state. When they are excited periodically over the spectrum, then due to interference of different spectrum components, the averaged response approximately cancels. This cancellation is clearly shown in transient nutation decay. The appearance of a nonoscillating component of the hole at a time $t=t_p$ gives a nonzero response. Thus the duration of the first pulse is stored in the spectrum and the second pulse reads it. The SNE arising during pulse II appears exactly at a time t_p after switching on of the pulse.

To demonstrate this we consider the solution of the simple optical Bloch equations

$$\begin{aligned} \dot{u}+\Delta v+u/T_2&=0,\\ \dot{v}-\Delta u-\chi w+v/T_2&=0,\\ \dot{w}+\chi v+(w-w_0)/T_1&=0, \end{aligned} \tag{1}$$

which follow from density-matrix equation of motion for a two-level particle. The Bloch vector amplitudes u, v, and w are related to the density-matrix elements by $\rho_{12}=\frac{1}{2}(u+iv)e^{i\Omega t}$, the dipole term, and $\rho_{22}-\rho_{11}=w$, the population difference term. We also define the tuning parameter $\Delta=\omega-\Omega$, where ω is the frequency splitting of the two-level particle and Ω is the driving field frequency. Specifically, we consider low-temperature solids where the dipole dephasing time T_2 is much shorter than the population decay time T_1.

Pulse I ($t_p \ll T_2, T_1$) burns a population-difference hole train described by expression

$$w(\Delta,t_p)=\left(\frac{\chi}{g}\right)^2(1-\cos g t_p)-1, \tag{2}$$

where $g^2=\Delta^2+\chi^2$ and the condition of $w_0=-1$ is implied. Considering the particles satisfying the condition $g t_p=\pi n$,

*Electronic address: shakhmuratov@ksc.iasnet.ru

one can recognize those that return to the ground state (when n is even) and those in the excited state (when n is odd). For a long delay time ($t_d \gg T_2$) between pulses, the dipole components u and v vanish. Therefore, at the moment of the switching on of pulse II ($t=0$), the particle states are determined only by the population difference

$$w(\Delta,t_p+t_d)=[w(\Delta,t_p)+1]\exp(-t_d/T_1)-1. \quad (3)$$

For excitation at the center of a symmetric, inhomogeneous absorption line $f(\Delta)$, the transient nutation signal induced by pulse II is described by [5]

$$\langle v(t)\rangle=\int_{-\infty}^{\infty} v(\Delta,t)f(\Delta)d\Delta, \quad (4)$$

where $v(\Delta,t)$ is a solution of Eqs. (1) with the initial condition (3). When $t \ll T_2, T_1$, we obtain

$$v(\Delta,t)=\frac{\chi}{g}\sin(gt)w(\Delta,t_p+t_d). \quad (5)$$

One can rewrite Eq. (5) as

$$v(\Delta,t)=-\frac{\chi}{g}\mathrm{sin}gt+\frac{\chi^3}{2g^3}[2\mathrm{sin}gt-\mathrm{sin}g(t+t_p) -\mathrm{sin}g(t-t_p)]\exp\left(-\frac{t_d}{T_1}\right) \quad (6)$$

and show that there are two kind of integrals in Eq. (4), i.e.,

$$\langle v(t)\rangle=-f(0)\left\{M_1(t)-(M_2(t)-\tfrac{1}{2}[M_2(t+t_p) +M_2(t-t_p)])\exp\left(-\frac{t_d}{T_1}\right)\right\}, \quad (7)$$

where

$$M_1(t)=\int_{-\infty}^{\infty}\frac{\chi}{g}\sin(gt)d\Delta, \qquad M_2(t)=\int_{-\infty}^{\infty}\left(\frac{\chi}{g}\right)^3\sin(gt)d\Delta, \quad (8)$$

and the distribution $f(\Delta)$ is taken to be flat. The Laplace transform

$$M_{1,2}(p)=\int_0^{\infty} M_{1,2}(t)\exp(-pt)dt\equiv\mathcal{L}\{M_{1,2}(t)\} \quad (9)$$

of these integrals are simple functions

$$M_1(p)=\frac{\pi\chi}{\sqrt{p^2+\chi^2}}, \qquad M_2(p)=\left(\frac{\chi}{p}\right)^2[\pi-M_1(p)]. \quad (10)$$

The inverse Laplace transform

$$M_1(t)=\mathcal{L}^{-1}\{M_1(p)\}\equiv\frac{1}{2\pi i}\int_{c-i\infty}^{c+i\infty}e^{ipt}M_1(p)dp \quad (11)$$

of the first is known [11], i.e.,

$$M_1(t)=\pi\chi J_0(\chi t), \quad (12)$$

where $J_0(x)$ is a zeroth-order Bessel function. The second function can be found by applying the convolution theorem [11]

$$\mathcal{L}^{-1}\{\Phi_1(p)\Phi_2(p)\}=\int_0^t\Phi_1(t-\tau)\Phi_2(\tau)d\tau. \quad (13)$$

The result is

$$M_2(t)=\pi\chi^2\left\{t-\chi\int_0^t(t-\tau)J_0(\chi\tau)d\tau\right\}. \quad (14)$$

Finally, we get the expression for transient response of the system on pulse II,

$$\langle v(t)\rangle=-\pi\chi f(0)\left[J_0(t')+\{K(t')-\tfrac{1}{2}[K(t'+T) +\mathrm{sgn}(t'-T)K(|t'-T|)]\}\exp\left(-\frac{t_d}{T_1}\right)\right], \quad (15)$$

where $\mathrm{sgn}(t'-T)$ is the sign of the difference $t'-T$, $t'=\chi t$, and $T=\chi t_p$. Below we shall sometimes drop the prime in the notation so that the time t is a dimensionless parameter and we drop the dependence on delay time t_d to simplify mathematical expressions. Here the function $K(t)$ is

$$K(t)=\int_0^t(t-\tau)J_0(\tau)d\tau=t[L(t)-J_1(t)], \quad (16)$$

$$L(t)=\int_0^t J_0(\tau)d\tau, \quad (17)$$

and $J_1(t)$ is a first-order Bessel function. Before analysis of the signal (15), let us consider the time derivative of the v component (5),

$$\dot{v}(\Delta,t)=\chi\cos(gt)w(\Delta,t_p). \quad (18)$$

Here time t is dimensional and $t_d \ll T_1$. This expression is similar to the $w(\Delta,t)$ component in its time t and t_p dependences as it contains the product $\cos(gt)\cos(gt_p)$. Therefore the hole interference is displayed much better in the derivative $\dot{v}(\Delta,t)$. The average value of the latter expression is

$$\langle\dot{v}(t)\rangle=\pi\chi^2 f(0)\{J_1(t)-L(t)+\tfrac{1}{2}[L(t+T)+L(|t-T|)]\} \quad (19)$$

(here time t is normalized). Transient effects become pronounced when the area of pulse I is large ($T \gg 1$). Noting that the asymptote of the function $L(t)$ at large t [11] is

$$\lim_{t\to\infty}L(t)=1, \quad (20)$$

while

$$\lim_{t\to\infty} J_1(t)=0, \tag{21}$$

one can estimate the value of Eq. (19) as nearly zero $[\langle\dot{v}(t)\rangle=0]$ for the conditions $t\gg1$ and $|t-T|\gg1$. When the time t coincides exactly with pulse duration T, the last term in square brackets of Eq. (19) equals zero and the derivative (19) takes on its maximum value of

$$\langle\dot{v}(T)\rangle\approx-\frac{\pi}{2}\chi^2 f(0). \tag{22}$$

To analyze the behavior of Eq. (19) near time $t=T$, we examine the $L(t)$ function for small t. This function rises from 0 up to 1 almost linearly for $0<t<1$. The value 1 is reached at $t\simeq1.108\,36$. Then this function oscillates slightly near the value 1 with a damped amplitude. Therefore the function (19) becomes zero near the maximum (22) whenever $L(|t-T|)=1$. This occurs at times $t_1\simeq T\pm1.1(08\,36)$, $t_2\simeq T\pm4.05$, $t_3\simeq T\pm7.15$, etc. (see [11]). The value (22) is an absolute maximum of the function (19), as the local maxima and minima of this function, lying between times t_i and t_{i+1}, are smaller by an absolute value. The time dependence of Eq. (19) for $T=9\pi$ is shown on Fig. 1(a). As the derivative of the signal approaches the absolute maximum value at $t=T$, the signal [Eq. (15)] undergoes the largest change near the time T attaining a maximum amplitude at $t\simeq T\pm1.1$. To obtain the signal value [Eq. (15)] at time $t=T$ and for times $|t-T|\gg1$ we consider the time dependence of the function (16). Taking into account the validity of the relations $K\simeq t$ at $t\gg1$ (see Appendix A) and $K(0)=0$ at $t=0$, one can show that Eq. (15) is nearly zero at $t\gg1$, $|t-T|\gg1$, and $t=T$. Thus the signal becomes zero for $t=T$. The dependence of Eq. (15) for $T=9\pi$ is shown on Fig. 1(b). By measuring the time interval t_{12} (nonnormalized) between the first absolute maximum and the first absolute minimum of the signal, one can determine the Rabi frequency, since the relation

$$\chi t_{12}\simeq2.22 \tag{23}$$

is valid.

To estimate the maximum amplitude of the signal at $t=t_1$ for large T we consider the function

$$\begin{aligned} F_0(t)&=F_1(t)+F_2(t),\\ F_1(t)&=J_0(t)+K(t)-\tfrac{1}{2}K(t+T),\\ F_2(t)&=-\tfrac{1}{2}\mathrm{sgn}(t-T)K(|t-T|), \end{aligned} \tag{24}$$

which describes the time dependence of the signal (15). Substitution of the asymptotes

$$J_0(t)=O_1(1/\sqrt{t}),\quad K(t)=t+O_2(1/\sqrt{t}) \tag{25}$$

for large t into the function $F_1(t)$ gives the result

$$F_1(t)=\frac{t-T}{2}+O_3(1/\sqrt{t}), \tag{26}$$

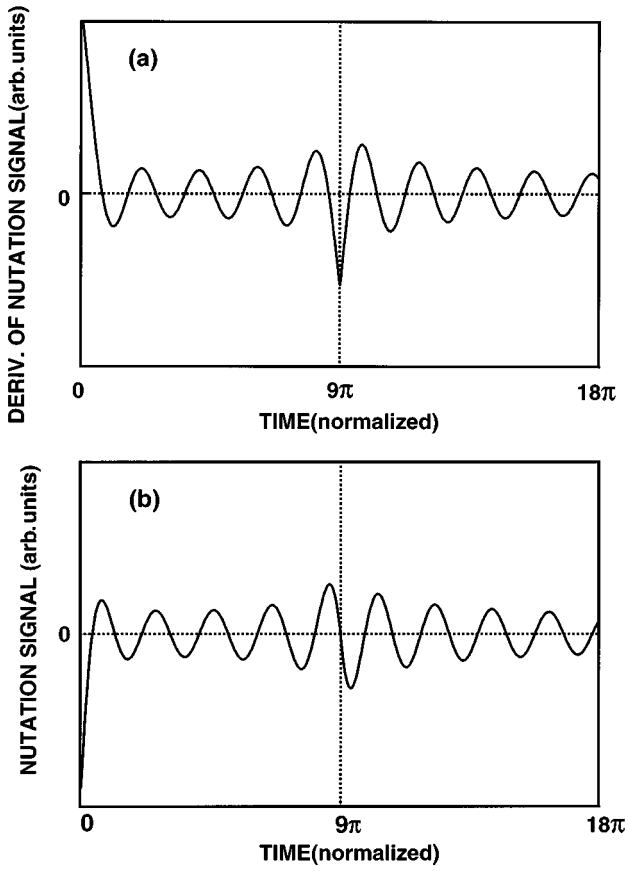

FIG. 1. (a) Calculated time dependence of the nutation signal derivative [plane-wave excitation, Eq. (19)]. Time is normalized as described in the text and zero time corresponds to the beginning of the second pulse. The first pulse width is $T=9\pi$. The nutation echo is centered at time T after the start of the second pulse. (b) Calculated time dependence of the nutation signal [derivative shown in (a)] for plane-wave excitation, Eq. (15).

where O_i is a small value of order $1/\sqrt{t}$. The second component $F_2(t)$ at the time $t_1=T\pm1.1(08\,360)$ equals

$$F_2(t_1)=\frac{(t_1-T)}{2}[J_1(|t_1-T|)-1]. \tag{27}$$

Combining both, we get the signal amplitude at time t_1

$$\begin{aligned} F_0(t_1)&=\pm\frac{1.108\,36}{2}J_1(1.108\,36)+O_3(1/\sqrt{t_1})\simeq\pm0.262,\\ \langle v(t_1)\rangle&\simeq\mp0.262\pi\chi f(0). \end{aligned} \tag{28}$$

In a similar way, one can estimate the amplitudes of the local maxima and minima at times t_i $(i>1)$. The echo amplitude is about 25–30% of the initial maximum of the nutation signal at $t=0$ [see Eq. (A6) in Appendix A].

Now we consider the signal measured by optical detector. The field

$$E_0(t)=E_0e^{i\Omega t}$$

induces a polarization

$$p(t)=i\frac{dN}{2}\langle v(t)\rangle e^{i\Omega_t}$$

in the sample, where d is a transition dipole matrix element and N is the impurity number density. This polarization excites the response field

$$E_r(t)=-i\frac{\Omega Nl}{\varepsilon_0 c}p(t),$$

where l is the length of the sample, which is assumed to be optically thin. The optical field reaching the detector is the sum of the laser field and the emitted sample field. Since the optical detector is a square law device, we must calculate the intensity present at the detector, which is

$$I(t)=c\varepsilon_0 E_S(t)E_S^*(t),$$

where $E_S(t)=E_0(t)+E_r(t)$. Now $E_r \ll E_0$ for any optically thin sample, so the term proportional to $|E_r|^2$ may be ignored and

$$I(t)=c\varepsilon_0(E_0^2+2E_0E_r).$$

Finally, we obtain

$$I(t)=I_0+\Omega NldE_0\langle v(t)\rangle, \tag{29}$$

where $I_0=c\varepsilon_0 E_0^2$.

Equation (29) was derived assuming plane-wave excitation. However, the laser beam has a Gaussian profile, which means that E_0 should be replaced by $E_0\exp(-R^2/2a^2)$, where a is the beam radius. Neglecting diffraction effects, the observed signal for a large area detector is then reduced to the integral of Eq. (29) over the beam profile,

$$S=2\pi\int_0^\infty I(t)R\,dR. \tag{30}$$

As will be shown later, this averaging of the Rabi frequency distribution over the beam profile increases the sharpness of the echo signal since, in addition to the hole interference in the resonant frequency domain, there is also a hole interference in the Rabi frequency domain. The result of the integral (30) calculation (see Appendix B) is

$$S=S_0\left[1-\frac{2\pi lN\Omega f(0)d^2}{c\varepsilon_0\hbar}F_3(t)\right], \tag{31}$$

where $S_0=\pi a^2 I_0$,

$$F_3(t)=\frac{J_1(t)}{t}+\{K_1(t)-\tfrac{1}{2}[K_1(t+T)+\mathrm{sgn}(t-T)K_1(|t-T|)]\}\exp(-t_d/T_1), \tag{32}$$

$$K_1(t)=\frac{1}{2}\int_0^t\left[\frac{2}{3}t-\tau\left(1-\frac{\tau^2}{3t^2}\right)\right]J_0(\tau)d\tau.$$

(Here time t is normalized.)

Analysis of Eqs. (31) and (32) is somewhat similar to that of Eq. (15) for the condition $t_d \ll T_1$. The function $K_1(t)$ is related to $K(t)$ as

$$3K_1(t)=K(t)-J_2(t), \tag{33}$$

whereas its time derivative is

$$\dot{K}_1(t)=\frac{1}{3}\left[L(t)-J_1(t)+2\frac{J_2(t)}{t}\right]. \tag{34}$$

Therefore, the derivative of the time-dependent part of the signal (31)

$$\dot{F}_3(t)=-\frac{J_2(t)}{t}+\dot{K}_1(t)-\frac{1}{2}[\dot{K}_1(t+T)+\dot{K}_1(|t-T|)] \tag{35}$$

is small for $t\gg 1$ and $|t-T|\gg 1$. It reaches a maximum value of 1/6 at the echo time $t=T$. The zeros nearest this maximum of the function $\dot{F}_3(t)$ occur at $t_1=T\pm 1.5142$ when $\dot{K}_1(|t-T|)=1/3$. Here the pulse area is assumed to be large ($T\gg 1$). The function $F_3(t)$ is small at $t\gg 1$, $|t-T|\gg 1$, as well as echo time $t=T$. The echo amplitude reaches its maximum value at $t_1=T\pm 1.5142$ when the derivative $\dot{K}_1(t)$ is zero. Its value is

$$F_3(t_1)=\pm\tfrac{1}{2}J_2(1.5142)+O_4(t_1),$$

where the last term is small, i.e.,

$$O_4(t_1)=\frac{\sin\left(t_1+T-\frac{\pi}{4}\right)}{\sqrt{2\pi(t_1+T)^3}}+\cdots.$$

The echo amplitude

$$\tfrac{1}{2}J_2(1.5142)=0.118$$

is about 24% of first nutation maximum

$$F_3(0)=1/2$$

and 2.637 times higher than the mean amplitude of the first minimum and second maximum of transient nutation oscillations. The time dependence of the $-F_3(t)$ and $-\dot{F}_3(t)$ functions for $T=9\pi$ is shown in Figs. 2(a) and 2(b).

Additional interference of holes in the Rabi frequency domain makes the echo signal much more pronounced, as it damps the oscillations far from the echo time $t=T$. The time interval t_{12} (nonnormalized) between maximum and minimum values of the signal becomes larger, i.e.,

$$t_{12}\chi=3.03.$$

This relation may be very useful for measurement of Rabi frequencies.

III. EXPERIMENT

Stimulated nutation echoes were excited in a ruby crystal by two optical pulses obtained by acousto-optic chopping of a cw laser beam (80 mW, focused to $\sim$0.1 mm diameter in the crystal) from a single frequency Ti:sapphire laser (Coher-

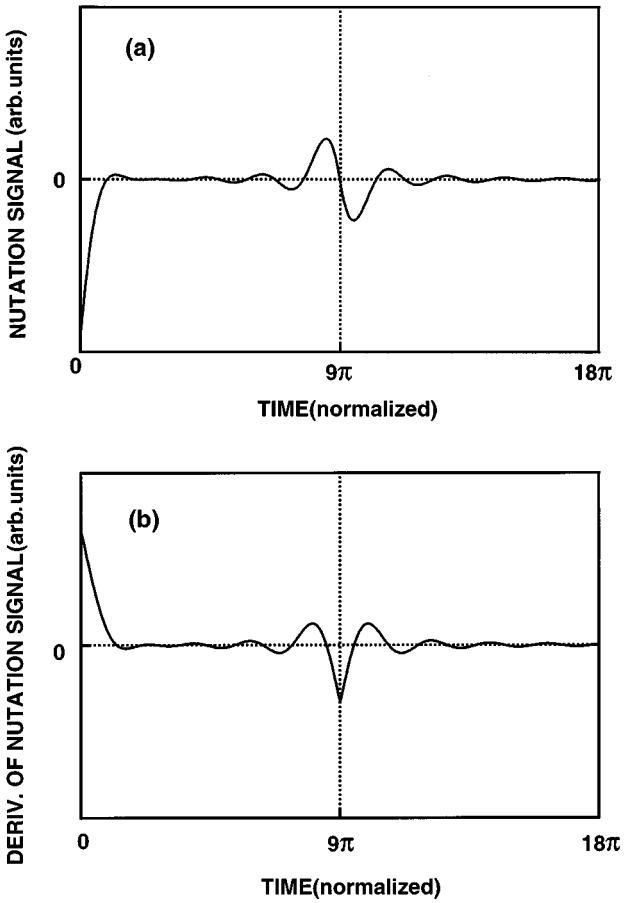

FIG. 2. (a) Calculated time dependence of the nutation signal [Gaussian beam excitation, $-F_3(t)$ function, Eqs. (31) and (32)]. Time is normalized as described in the text and zero time corresponds to the beginning of the second pulse. The first pulse width is $T=9\pi$. The nutation echo is centered at time T after the start of the second pulse. (b) Derivative of the curve in (a).

ent 899-21). The sample was 1.58 mm thick with a 0.0034 wt. $\%Cr_2O_3$ concentration. It was located in a magnetic field of 7.5 kG aligned along the c axis and maintained at a temperature of 2.0 K by a Lakeshore model DRC-93CA controller. The $^4A_2(-3/2)\rightarrow\bar{E}(-1/2)$ transition of Cr^{3+} was selectively excited by the circularly polarized laser beam. The transmitted beam was detected by a photodiode and the signal was processed by a low noise amplifier (Stanford SR560) followed by display on a Lecroy 9354 digital oscilloscope (500 MHz bandwidth) after averaging 300 sweeps.

The detected two pulse sequence is shown in Fig. 3, which clearly shows the SNE during the second pulse. Analysis of the data indicates that the SNE occurs very near the expected time t_p after the onset of the second pulse. A slight shift from t_p occurs because of the finite rise and fall time of the pulses. This behavior has also been simulated by numerical studies.

We verified the influence of finite rise and fall time for the first pulse on echo signal. By numerical calculations [12] we found that the echo, induced by the pulse edges, was very small (one to two orders smaller than the normal nutation) and very sharp in time (about rise time), which did not agree with experiment.

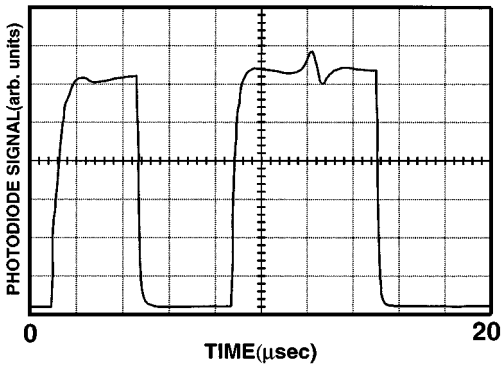

FIG. 3. Experimental observation of the nutation echo. The signal shows the transmitted light through the sample. The first pulse (width $t_p=4.5$ μsec) is followed by a probe pulse with the echo centered at time t_p following the start of the probe pulse.

IV. DISCUSSION AND CONCLUSION

One application of the SNE is for Rabi frequency measurement using the relation $\chi t_{12}=3.03$ derived above for a Gaussian-shaped beam. This application is particularly advantageous over conventional nutation at lower Rabi frequencies where rapid damping will prevent clear observation of the ringing. Also, the SNE provides a larger signal than the leading edge nutation (for pulse I, see Fig. 3).

The ''stimulated'' or hole-burning origin of the SNE is demonstrated by the experimental decay plot shown in Fig. 4. The echo decay closely resembles that seen for three-pulse-stimulated echoes [13] for this sample [14] in that there is an initial fast decay followed by a slow decay of the form $\exp(-t_d/T_1)$ due to population relaxation. The fast decay is caused by spectral diffusion. As the frequency spacing between adjacent dips in the hole pattern burnt by the first pulse depends on pulse duration and Rabi frequency, the frequency range over which diffusion occurs can be studied by varying these parameters.

This frequency range may be estimated as follows. Adjacent maximum and minimum values of population difference, burnt by the first pulse, are separated by frequency

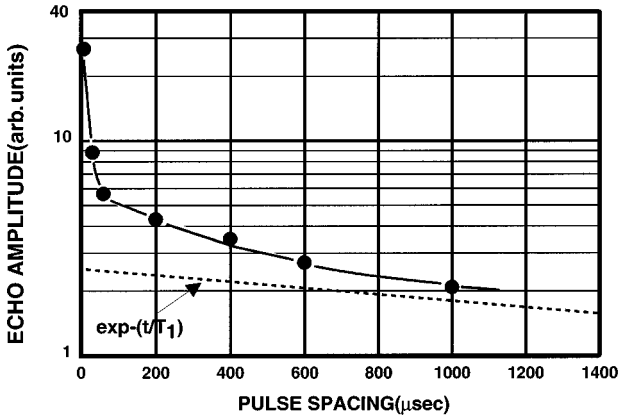

FIG. 4. Experimental echo amplitude dependence on pulse spacing. At long times, the echo time dependence approaches the expected function $\exp-(t/T_1)$, where T_1 is the spontaneous lifetime. The fast initial decay is due to spectral diffusion (see the text).

Δ. For the central frequency packets this Δ satisfies the relation

$$(\sqrt{\chi^2+\Delta^2}-\chi)t_p=\pi.$$

When $|\Delta|<\chi$, this relation simplifies to

$$\Delta\simeq\chi\sqrt{\frac{2\pi}{\chi t_p}}.$$

If $\chi t_p=\pi n$ (the echo is well recognized when $n\geqslant 3$), then

$$\Delta\simeq\chi\sqrt{\frac{2}{n}}. \tag{36}$$

If due to spectral diffusion the particles move over the spectrum for a distance larger than Δ, then the echo vanishes. We are planning to discuss this question in a forthcoming paper.

ACKNOWLEDGMENTS

R.N. expresses his thanks to the Program on the Physics of Quantum and Wave Processes; Trend: Fundamental spectroscopy (Project No. 4.8). A.S. acknowledges the fine technical support of J. Froemel.

APPENDIX A

Noting the relation $L(\infty)=1$, we transform Eq. (16) to

$$K(t)=t\left[1-J_1(t)-\int_t^\infty J_0(\tau)d\tau\right]. \tag{A1}$$

For large t, we use the Bessel-function asymptote

$$J_n(t)=\sqrt{2/\pi t}\{P(n,t)\cos\alpha-Q(n,t)\sin\alpha\}, \tag{A2}$$

where $\alpha=t-(\pi/4)(2n+1)$,

$$\begin{aligned}
P(n,t)&=\sum_{k=0}^{\infty}(-1)^k\frac{(n,2k)}{(2t)^{2k}},\\
Q(n,t)&=\sum_{k=0}^{\infty}(-1)^k\frac{(n,2k+1)}{(2t)^{2k+1}},\\
(n,m)&=\frac{\Gamma(\frac{1}{2}+n+m)}{m!\Gamma(\frac{1}{2}+n-m)},\\
\Gamma(\tfrac{1}{2}+n)&=\frac{\sqrt{\pi}}{2^n}(2n-1)!!,\\
\Gamma(\tfrac{1}{2}-n)&=(-1)^n\frac{2^n\sqrt{\pi}}{(2n-1)!!},\\
(2n-1)!!&=1\times3\times5\times\cdots\times(2n-1).
\end{aligned} \tag{A3}$$

For example, the coefficients (A3) for Bessel functions $J_0(t)$ and $J_1(t)$ are approximated by

$$P(0,t)=1-\frac{9}{128t^2}+\cdots,\quad Q(0,t)=-\frac{1}{8t}+\cdots, \tag{A4}$$

$$P(1,t)=1+\frac{15}{128t^2}+\cdots,\quad Q(1,t)=\frac{3}{8t}+\cdots.$$

Substitution of the approximation (A2) with coefficients (A4) into the expression (A1) gives the result

$$K(t)=t+O_2(1/\sqrt{t}), \tag{A5}$$

where

$$O_2(1/\sqrt{t})=-\sqrt{\frac{2}{\pi t}}\left[\cos\left(t-\frac{\pi}{4}\right)+\frac{9}{8t}\sin\left(t-\frac{\pi}{4}\right)\right]+\cdots$$

is a small value of order $1/\sqrt{t}$. We calculated the $O_3(1/\sqrt{t_1})$ term in Eq. (26) and obtained an improved, approximate expression for maximum and minimum values of $F_0(t)$,

$$\begin{aligned}
F_0(t_1)&=\pm0.262+O_3(1/\sqrt{t_1}),\\
O_3(1/\sqrt{t_1})&=\frac{1}{\sqrt{2\pi(T+t_1)}}\left[\cos\left(T+t_1-\frac{\pi}{4}\right)\right.\\
&\quad\left.+\frac{9}{8(T+t_1)}\sin\left(T+t_1-\frac{\pi}{4}\right)\right]\\
&\quad-\sqrt{\frac{2}{\pi t_1^3}}\sin\left(t_1-\frac{\pi}{4}\right)+\cdots,
\end{aligned}$$

where $t_1=T\pm1.108\ 36$.

APPENDIX B

Expression (30) is reduced to three kinds of integrals,

$$S=2\pi a^2[I_0s_1-\pi lN\hbar\Omega f(0)B(t)],$$

$$B(t)=s_2(t)+s_3(t)-\tfrac{1}{2}[s_3(t+t_p)+\mathrm{sgn}(t-t_p)s_3(|t-t_p|)],$$

$$s_1=\int_0^\infty e^{-2y}dy=\tfrac{1}{2},\quad s_2(t)=\chi^2\int_0^\infty e^{-2y}J_0(\chi te^{-y})dy,$$

$$s_3(t)=\chi^4\int_0^\infty\int_0^t e^{-4y}(t-\tau)J_0(\chi\tau e^{-y})d\tau dy,$$

where $y=R^2/2a^2$ and $\chi=dE_0/\hbar$. By variables substitution of $x=\chi te^{-y}$ and $x'=\chi\tau e^{-y}$, the second and third integrals are transformed as

$$s_2(t)=\frac{1}{t^2}\int_0^{\chi t}xJ_0(x)dx=\frac{\chi}{t}J_1(\chi t),$$

$$s_3(t)=\frac{1}{t^2}\int_0^{\chi t}xK(x)dx,$$

where

$$K(x)=\int_0^x(x-x')J_0(x')dx'.$$

We calculated $s_3(t)$, integrating it in parts two times. The result is

$$s_3(t)=\frac{1}{t^2}\left\{\frac{x^2}{2}K(x)\Big|_0^{\chi t}-\int_0^{\chi t}\frac{x^2}{2}\dot{K}(x)dx\right\},$$

$$s_3(t)=\frac{\chi^2}{2}\int_0^{\chi t}\left\{\frac{2}{3}\chi t-x\left[1-\frac{x^2}{3(\chi t)^2}\right]\right\}J_0(x)dx.$$

[1] G. B. Hocker and C. L. Tang, Phys. Rev. Lett. **21**, 591 (1968); Phys. Rev. **184**, 356 (1969).

[2] R. G. Brewer and R. L. Shoemaker, Phys. Rev. Lett. **27**, 631 (1971).

[3] G. L. Tang and B. D. Silverman, *Physics of Quantum Electronics*, edited by P. Kelley, B. Lax, and P. Tannenwald (McGraw-Hill, New York, 1966), p. 280.

[4] R. L. Shoemaker and E. W. Van Stryland, J. Chem. Phys. **64**, 1733 (1976).

[5] R. L. Shoemaker, in *Laser and Coherence Spectroscopy*, edited by J. I. Steinfeld (Plenum, New York, 1978).

[6] J. Schmidth, P. R. Berman, R. G. Brewer, Phys. Rev. Lett. **31**, 1103 (1973).

[7] P. R. Berman, J. M. Levy, and R. G. Brewer, Phys. Rev. A **11**, 1668 (1975).

[8] R. G. Brewer and A. Z. Genack, Phys. Rev. Lett. **36**, 959 (1976).

[9] A. Schenzle and R. G. Brewer, Phys. Rev. A **14**, 1756 (1976).

[10] V. S. Kuz'min, A. P. Saiko, and G. G. Fedoruk, Zh. Éksp. Teor. Fiz. **99**, 215 (1991) [Sov. Phys. JETP **72**, 121 (1991)].

[11] *Handbook of Mathematical Functions*, Nat. Bur. Stand. Appl. Math. Ser. No. 55, edited by M. Abramowitz and I. A. Stegun (U.S. GPO, Washington, DC, 1964).

[12] A. Szabo and T. Muramoto, Phys. Rev. A **37**, 4040 (1988).

[13] S. Nakanishi, O. Tamura, T. Muramoto, and T. Hashi, Jpn. J. Appl. Phys. **19**, L57 (1980).

[14] A. Szabo (unpublished).